Mutation of the Iron Ligand His 249 to Glu in the N-Lobe of Human Transferrin Abolishes the Dilysine "Trigger" but Does Not Significantly Affect Iron Release † , ‡

7 AUTHORS, INCLUDING:

Clyde A Smith
Stanford University
92 PUBLICATIONS   3,219 CITATIONS
SEE PROFILE

Anne B Mason
University of Vermont
121 PUBLICATIONS   3,364 CITATIONS
SEE PROFILE

Robert C Woodworth
University of Vermont
101 PUBLICATIONS   3,090 CITATIONS
SEE PROFILE

Edward N Baker
University of Auckland
154 PUBLICATIONS   8,266 CITATIONS
SEE PROFILE

Mutation of the Iron Ligand His 249 to Glu in the N-Lobe of Human Transferrin Abolishes the Dilysine "Trigger" but Does Not Significantly Affect Iron Release[†,‡]

Ross T. A. MacGillivray,[§,||] Maria C. Bewley,[§,⊥] Clyde A. Smith,[#] Qing-Yu He,[▽] Anne B. Mason,[▽] Robert C. Woodworth,[▽] and Edward N. Baker*[,§,#]

Department of Biochemistry, Massey University, Palmerston North, New Zealand, Department of Biochemistry & Molecular Biology, University of British Columbia, Vancouver, Canada V6T 1Z3, Department of Biochemistry, University of Vermont, Burlington, Vermont 05405, USA, School of Biological Sciences, University of Auckland, Auckland, New Zealand

ABSTRACT: Serum transferrin is the major iron transport protein in humans. Its function depends on its ability to bind iron with very high affinity, yet to release this bound iron at the lower intracellular pH. Possible explanations for the release of iron from transferrin at low pH include protonation of a histidine ligand and the existence of a pH-sensitive "trigger" involving a hydrogen-bonded pair of lysines in the N-lobe of transferrin. We have determined the crystal structure of the His249Glu mutant of the N-lobe half-molecule of human transferrin and compared its iron-binding properties with those of the wild-type protein and other mutants. The crystal structure, determined at 2.4 Å resolution (*R*-factor 19.8%, R_{free} 29.4%), shows that Glu 249 is directly bound to iron, in place of the His ligand, and that a local movement of Lys 296 has broken the dilysine interaction. Despite the loss of this potentially pH-sensitive interaction, the H249E mutant is only slightly more acid-stable than wild-type and releases iron slightly faster. We conclude that the loss of the dilysine interaction does make the protein more acid stable but that this is counterbalanced by the replacement of a neutral ligand (His) by a negatively charged one (Glu), thus disrupting the electroneutrality of the binding site.

Serum transferrin is an iron-binding protein which, together with lactoferrin and ovotransferrin, is part of a homologous family of proteins known collectively as the transferrins (for reviews, see refs *1* and *2*). Because of their extremely high affinity for iron, the transferrins play a crucial part in regulating the levels of free iron in the body fluids of animals. Additionally, serum transferrin has the specific role of iron transport in the bloodstream. Iron-loaded transferrin binds to specific cellular receptors, after which a process of receptor-mediated endocytosis allows the iron to be released inside the cell, and the iron-free transferrin to be returned to circulation (*3*). Critical to this process is the ability of transferrin to bind iron with high affinity, yet to possess mechanisms that permit its release. Our goal is to understand both the origin of the very high affinity of

transferrins for iron and the molecular events that lead to its release.

In serum transferrin, as in other transferrins, the amino acid sequence contains an internal 2-fold sequence repeat (*4*), such that the N-terminal half has ca. 40% sequence identity with the C-terminal half. Correspondingly, crystallographic studies of transferrin (*5*), lactoferrin (*6*, *7*), and ovotransferrin (*8*) have shown that each protein is folded into two globular lobes of extremely similar structure, with each lobe possessing a single iron-binding site. The iron-binding sites, too, are extremely similar, with the same ligands bound to iron in every case. Thus, half-molecule fragments, obtained by expression of recombinant proteins, have proved extremely useful as models to analyze the factors governing iron binding and release (e.g., refs *9−15*).

The canonical transferrin iron-binding site, found in each lobe of Tf, Lf, and Otf, lies in a deep cleft between two similar domains. Four ligands are provided by the protein, comprising one aspartic acid residue, two tyrosine residues, and one histidine residue; in the N-lobe of human transferrin, these four ligands are Asp 63, Tyr 95, Tyr 188, and His 249. Two remaining coordination positions round the iron are filled by oxygen atoms of a synergistically bound carbonate ion, which binds as a bidentate ligand. The high affinity for iron, as Fe(III), probably derives from a number of factors, including the preference of Fe(III) for negatively charged

[1] Abbreviations: Tf, serum transferrin; Lf, lactoferrin; Otf, ovotransferrin; hTf/2N, recombinant N-lobe half-molecule of human transferrin, residues 1−337; H249E, His249Glu mutant of hTf/2N; BHK cells, baby hamster kidney cells; NTA, nitrilotriacetate; rms, root-mean-square.

oxygen ligands, and the near-perfect match of charge and size within the binding site. The 3+ charge of the ferric ion is matched by the negative charges of the carboxylate and two phenolate ligands, and the negative charge of the carbonate ion is balanced by positive charge on the protein, contributed by an arginine residue (Arg 124 in the N-lobe of human transferrin) and the N-terminus of an α-helix (2).

The factors that govern iron release from transferrins are the subject of much debate. Structurally, it is known that iron release is accompanied by a major conformational change, in which the two domains that enclose the binding site move apart through a hinge motion, one domain rotating 55−65° relative to the other (16, 17). What triggers this movement is less clear. The transferrin receptor may play an active part in vivo (18), but iron is also released in vitro as the pH is lowered and this is believed to help effect iron release at the lower intracellular pH. The crystal structure of the N-lobe half-molecule of human transferrin, in its iron-bound state, showed two alternative positions for the carbonate ion; these two positions were interpreted in terms of a mixture of carbonate and bicarbonate at the crystal pH of ca. 6.0, indicating that protonation of the anion was a likely first step in iron release (15). Protonation of the histidine ligand as the pH is lowered is also a possible contributor (16, 19). Other factors, involving second-shell residues, must also play a part, however, since the primary iron coordination spheres in the N- and C-lobes, and in different transferrins, appear to be structurally identical, yet their iron release properties differ. The N-lobe of human transferrin, for example, releases iron below pH 6, about one pH unit higher than the C-lobe and two pH units higher than either lobe of lactoferrin. One intriguing structural feature that is proposed to be responsible for these differences is a hydrogen-bonded pair of lysine residues (Lys 206 and Lys 296 in human transferrin) that is present in the N-lobes of transferrin (5, 10) and ovotransferrin (8, 20) but not in their C-lobes, nor in lactoferrin. The two lysines come from opposing domains and lie immediately behind the iron site, leading to the suggestion that they form a pH-sensitive "dilysine trigger" (20).

We have chosen to investigate the influence of the histidine ligand of human transferrin on iron binding and release, through a combination of site-directed mutagenesis, spectroscopy, and structural analysis, using the recombinant N-lobe of human transferrin as our experimental system. Kinetic studies of the H249A, H249Q, and H249E mutants are presented separately (21); here we report the crystal structure of the H249E mutant. This has allowed us to evaluate the effects of substituting a negatively charged ligand (Glu) for the neutral histidine, thus disrupting the electroneutrality of the site, and at the same time has uncovered an unexpected disruption of the dilysine interaction which has important implications for understanding the stability of the iron-binding site.

MATERIALS AND METHODS

Mutations of His249 to Glu, Gln, and Ala were introduced into the gene for the N-terminal half-molecule of human transferrin (residues 1−337 of the native protein) using a polymerase chain reaction (PCR) based procedure, as described (21). The mutant proteins (H249E, H249Q, and H249A), together with the parent wild-type half-molecule hTf/2N, were then expressed in baby hamster kidney (BHK) cells, using the pNUT vector (22), and purified from the tissue culture medium, using modifications that have been described in detail (21).

Iron Binding and Release. For the analysis of the pH dependence of iron release, each protein was first titrated with sufficient 0.01 M ferric nitrilotriacetate solution to fully saturate its iron-binding capacity, as described previously (10). Samples of the Fe(III)-loaded proteins were then incubated, in the presence and absence of chloride ([KCl] = 0.14 M), against a series of buffers, chosen to give appropriate buffering over the pH range 7.7 to 4.2. Each of the proteins was at a concentration of approximately 78 μM and in its normal carbonate complex form. The buffers used were Hepes, Mes, and sodium acetate, each at a concentration of 33 mM, adjusted to the appropriate pH with 1 M NaOH or acetic acid. Each solution was maintained at 4 °C for a period of 1 week at the appropriate pH to achieve equilibrium. The percent saturation with iron was then estimated from the visible absorption spectrum, by comparing the absorbance at the visible absorption maximum (472, 430, 457, and 442 nm, respectively, for wt hTf/2N, H249A, H249E, and H249Q proteins) with that of the fully iron-loaded protein. All UV−vis spectra were recorded on a Cary 219 spectrophotometer under the control of the computer program Olis-219s (On-line Instrument Systems Inc., Bogart, GA).

Crystallization of the H249E Mutant. Fe(III)-saturated H249E was dialyzed against 20 mM sodium bicarbonate (pH 8.1) and concentrated to 80 mg/mL using a Centricon 10 Microconcentrator. Orange-colored crystals were obtained at 4 °C, using the sitting drop method in microbridges. The drop contained 1.5 μL of 50 mM potassium cacodylate buffer (pH 6.1), containing 40% (v/v) ethanol. The reservoir contained 40% (v/v) ethanol in 50 mM potassium cacodylate buffer in the pH range 5.9−6.3.

Data Collection. X-ray diffraction data for H249E were collected at room temperature, from a single crystal, using a Rigaku R-Axis IIC image plate detector on a Rigaku RU200 rotating anode generator. The crystal was found to belong to the tetragonal system and to be isomorphous to crystal form II of the wild-type hTf/2N, grown under similar conditions (15). Unit cell dimensions were $a = b = 72.66$, $c = 152.49$ Å, space group $P4_12_12$. Assuming one molecule of 37 kDa in the asymmetric unit the solvent content is 55%. A data set that was 91.2% complete to 2.4 Å resolution (96.1% complete in the outer, 2.6−2.4 Å, shell) was collected. The diffraction images were processed using the program DENZO (23) and subsequently scaled and merged using the programs ROTAVATA and AGROVATA from the CCP4 suite of programs (24). Full data collection statistics are in Table 1.

Structure Solution and Refinement. Because the H249E crystals were isomorphous with those of crystal form 2 of the wild-type half-molecule (hTf/2N), the final hTf/2N structure was placed directly into the H249E cell and used as the starting model for refinement. The iron ligands and second shell residues, together with the iron and carbonate ions and all solvent molecules, were omitted from this starting model. Initial refinement was with X-PLOR (25), with a round of rigid body refinement (first as one body,

Table 1: H249E Data Collection, Refinement, and Model Statistics

data collection	
resolution range (Å)	40.0−2.4
unique reflections	15 387
redundancy	4.7 (2.8)
completeness (%)	91.8 (96.1)
merging R-factor	0.079 (0.239)
mean I/σ	11.6 (5.6)
refinement	
resolution range (Å)	15.0−2.4
R-factor (no. of reflections)	0.198 (13 706)
Rfree (no. of reflections)	0.294 (1028)
rms deviation bond lengths (Å)	0.009
rms deviation bond angles (degrees)	1.68
model	
no. of protein atoms	2563
ions	1 Fe^{3+}, 1 CO_3^{2-}
no. of solvent molecules	67

then as the two domains) followed by simulated annealing and positional refinement with restrained isotropic B-factors. The stereochemical parameters of Engh and Huber (*26*) were used throughout. The omitted residues and ferric and carbonate ions were rebuilt into the model from $2F_{obs} - F_{calc}$ and $F_{obs} - F_{calc}$ maps using O (*27*) and late in the refinement solvent molecules were added conservatively, i.e., only if they appeared as discrete spherical peaks in both $2F_{obs} - F_{calc}$ and $F_{obs} - F_{calc}$ maps, at levels above 1.0σ and 3.0σ, respectively, and their positions made chemical and geometrical sense. All data in the resolution range 15−2.4 Å were used in the refinement, except that 7% of reflections, randomly chosen, were excluded for use in the R_{free} calculation. The final R-factor was 19.8% (R_{free} 29.4%) for a model in which the rms deviation from standard bond lengths was 0.009 Å. Full refinement statistics are in Table 1.

Final Model for H249E. The final model comprises 2563 protein atoms, one Fe^{3+} and one CO_3^{2-} ion, and 67 solvent molecules, all treated as water. The protein model comprises 331 residues out of the expected 337, as no interpretable density was found for residues 1−3 or 335−337. The rest of the model conforms well with standard geometry with 87% of residues in most favored regions of the Ramachandran plot, as defined in the program PROCHECK (*28*).

RESULTS AND DISCUSSION

Structure of the H249E Mutant. The overall structure of the H249E mutant has the same two-domain fold as in other transferrin half-molecules (*13−15, 20, 29*), with the iron-binding site and the mutated residue 249 located deep in the interdomain cleft, close to the two extended polypeptide strands that run between the domains (Figure 1). These strands contain the hinge that mediates domain opening and closure. Superposition of the whole polypeptide chain of H249E (331 Cα atoms, from residues 4 to 334) on to that of the wild-type hTf/2N gives an overall rms difference of 0.24 Å. When the individual domains are compared, superimposing domain 1 of H249E on to domain 1 of hTf/2N and domain 2 on to domain 2, the figures are almost the same as for the whole molecule, 0.22 and 0.23 Å respectively. We conclude that neither the overall fold nor the way in which the two domains close over the iron-binding site, are affected by the mutation or its local consequences. This is a significant finding in view of the fact that some of the interdomain contacts are changed (see below).
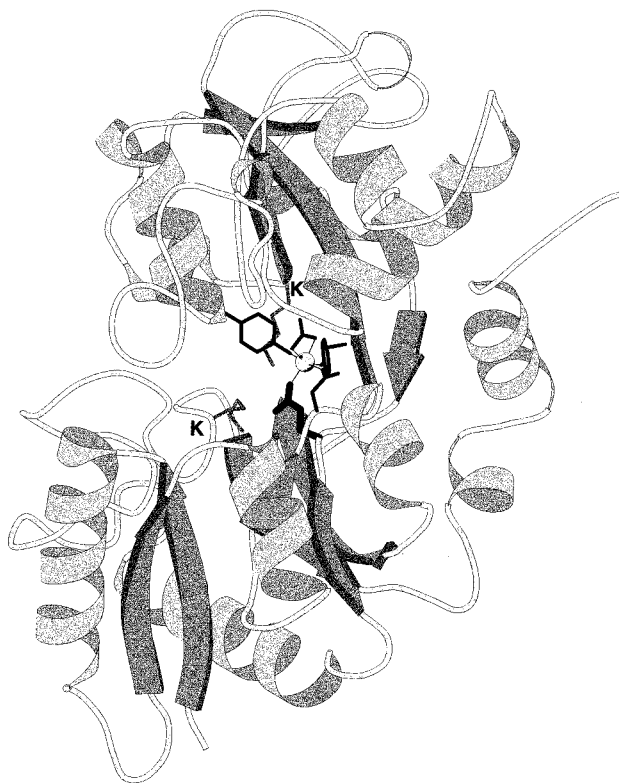

FIGURE 1: Ribbon diagram showing the overall folding of the H249E mutant and the location of the iron-binding site. In this orientation, the N2 domain is at the top of the picture and the N1 domain at the bottom. The mutated Glu 249 side chain is shown with thick lines and bound to the iron atom, and the nearby Lys 206 and Lys 296 side chains are indicated with the letter K; Lys 206 belongs to the N2 domain and Lys 296 to the N1 domain. This and other diagrams drawn with MOLSCRIPT (*36*), and rendered with RASTER3D (*37*).

At the mutation site, there are two particularly important changes. First, the mutated side chain, Glu 249, is directly bound to the iron atom (Figure 2), its carboxylate oxygen $O\epsilon2$ being coordinated with an Fe−O bond distance of 2.09 Å. This compares with the wild-type protein, in which His249 is coordinated through $N\epsilon2$ with an Fe−N distance of 2.04 Å. The coordination of the mutated glutamate residue in H249E is accommodated with minimal disturbance to the structure. Superposition of H249E on to wild-type hTf/2N shows that Glu 249 $O\epsilon2$ is within 0.5 Å of the position previously occupied by His249 $N\epsilon2$, and that the main-chain torsion angles for residue 249 remain essentially the same [changed from (−68°,151°) to (−80°,150°)]. The bond lengths (Table 2) suggest that the two Fe−O(Tyr) bonds are slightly shorter in H249E, compared with wild-type, although at 2.4 Å resolution the significance of this is uncertain. The bond distances of the other ligands are not changed significantly (Table 2), and the conformations of the carbonate ion and Arg 124 correspond to the normal high-pH configuration of the wild-type protein (*15*); there is no evidence of partial anion dissociation.

Coordination of Glu 249 is not in itself a surprise, since carboxylate ligands are common for Fe(III) in other non-heme iron proteins (*30*) and hard O^- ligands should be favorable for coordination to the Fe^{3+} ion. The effect, however, is that although the iron atom remains 6-coordinate, as in the wild-type protein, the introduction of a negatively
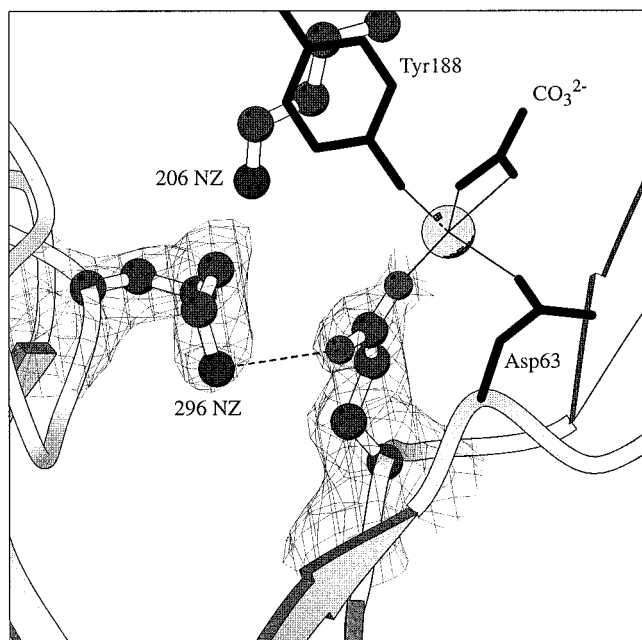
FIGURE 2: Electron density for the side chains of Glu 249 and Lys 296 showing that Glu 249 binds to the iron atom through one carboxylate oxygen and is hydrogen bonded (broken line) to the amino group of Lys 296, which has moved away from the position it occupies in the wild-type protein (adjacent to Lys 206 Nζ).

Table 2: Bond Distances at the Iron-Binding Site (Å)

	H249E	hTf/2N
Fe−Oδ1 (Asp 63)	2.11	2.03
Fe−Oη (Tyr 95)	1.60	1.97
Fe−Oη (Tyr 188)	1.65	1.88
Fe−Oϵ2 (Glu 249)	2.09	2.04 (His 249 Nϵ2)
Fe−O1 (carbonate)	1.99	2.08
Fe−O2 (carbonate)	1.97	2.19

charged ligand in place of the neutral His does change the electroneutrality of the site, with it now having a net negative charge. This is likely to affect the stability of iron binding.

The second change resulting from the mutation was not anticipated. The side chain of Lys 296, which in hTf/2N and other transferrin N-lobe structures is part of the hydrogen-bonded dilysine pair formed with Lys 206, has moved to form a hydrogen bond (2.97 Å) to the noncoordinated carboxylate oxygen, Oϵ1, of Glu 249 (Figure 2). In doing so, it replaces a water molecule that is bound to His 249 Nδ1 in wild-type hTf/2N. The new position appears to be a highly favorable one, as it also allows Lys 296 to make a hydrogen-bonded salt bridge (3.13 Å) with Glu 83 and another hydrogen bond with a well-ordered internal water molecule. This movement has the effect of breaking the dilysine interaction, as the two amino groups are now 7.8 Å apart, and a water molecule fills the position vacated by Lys 296 Nζ (Figure 3). The movement of Lys 296 has two other consequences that may be of significance. First, a common feature in proteins of the transferrin family is that in almost all cases a positively charged group, Lys 296 in transferrins and Arg 210 in human lactoferrin, sits behind the two tyrosine ligands, usually hydrogen bonded to Tyr 188 or its equivalent, so as to help maintain them in their deprotonated, phenolate, state. In H249E, this is no longer the case as the position is occupied by a water molecule. Second, the interdomain interactions are changed, as Lys 206, instead

of hydrogen bonding to Lys 296 is now hydrogen bonded only to Ser 298 Oγ from the opposing domain.

We emphasize, however, that the structural changes that result from the mutation are local ones that are not visibly propagated elsewhere in the molecule. The glutamate side chain almost exactly fills the position of the histidine in the wild-type protein, with Oϵ2 replacing Nϵ2 and Oϵ1 replacing Nδ1 (Figure 3). Likewise, the network of hydrogen bonds is unchanged by the substitution and by the movement of Lys 296 since the sites occupied by Lys 296 Nζ in the two proteins are alternatively occupied by water molecules. Instead, it is the *nature* of the bonded and hydrogen-bonded interactions that changes.

Iron-Binding Properties. Several kinds of data have been obtained on the iron-binding properties of the His 249 mutants (*21*). First, the wavelength, λ_{max}, of the charge-transfer band in the visible region gives an indication of any changes to the bonding of the two tyrosine ligands. For the carbonate complexes of the H249Q and H249A mutants, λ_{max} is reduced from 472 nm (wild-type) to 440 and 430 nm respectively, implying a relatively stronger interaction with the tyrosine ligands, perhaps as a result of the loss of the histidine ligand (*21*). For H249E, the reduction is less (to 457 nm). The crystal structure does suggest a slight shortening of the Fe−O(Tyr) bonds, as noted above and in Table 2, but its significance is marginal at 2.4 Å resolution. Second, iron release kinetics, using either Tiron or EDTA as chelators to effect iron removal, indicate dramatic differences in the rates of iron release from the mutants (*21*). Although the difference is small for the H249E mutant (about three times faster than wild-type), it is very large for the H249Q and H249A mutants for which the rate of iron release is some 10^4 times faster. These kinetic data reflect aspects of the mechanism of iron release that are affected by the mutations, however, and do not necessarily correlate with thermodynamic or acid stability. They may depend on the presence of binding sites for the chelators and/or other anions, for example, as well as the overall site stability.

The measurements of iron binding as a function of pH, shown in Figure 4, offer on the other hand a measure of the pH stability of iron binding without relating to other aspects of the mechanisms of release. These measurements offer an intriguing contrast. They show consistently, both in the presence and absence of chloride, that the H249E mutant is marginally more stable under acidic conditions than wild-type hTf/2N, whereas H249Q and H249A are significantly less stable (by about 1 pH unit). There is no inherent contradiction between the greater acid stability of the H249E mutant and its slightly faster release than wild-type because of the different nature of the two measurements, but interpretation is still difficult because of the fact that a number of factors are likely to be operating.

Considering the H249E mutant, we can advance several hypotheses. If protonation of the His ligand is a factor in the pH-dependent release of iron, as suggested (*16, 19*), then iron binding by H249E should be more acid stable (as observed). Likewise, if protonation of the dilysine pair in the N-lobe of transferrin is responsible for the dramatically reduced acid stability of the N-lobe-binding site compared with the C-lobe binding site, and with lactoferrin, as suggested (*20*), then one would expect the H249E mutant to
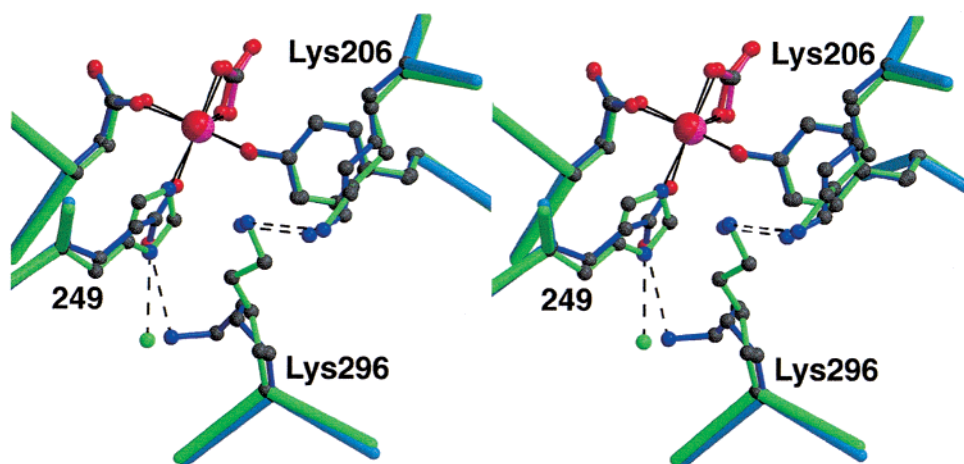
FIGURE 3: Superposition of the H249E mutant structure (blue polypeptide, red iron and carbonate) on to the wild-type hTf/2N structure (green polypeptide, magenta iron and carbonate) showing the change in conformation of the Lys 296 side chain that breaks the hydrogen-bonded interaction between Lys 296 and Lys 206 present in hTf/2N. Lys 296 NZ in H249E replaces a water molecule (green) in hTf/2N. Likewise the position vacated by Lys 296 NZ is filled by a water molecule (blue) hydrogen bonded to Lys 206 NZ. Hydrogen bonds are shown with broken lines.
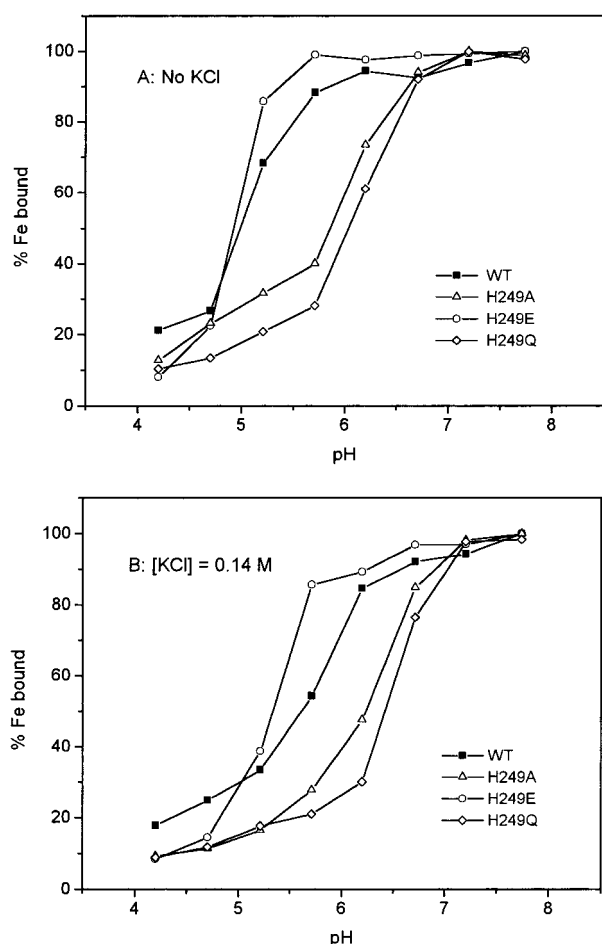

FIGURE 4: Plots of the percent of iron bound as a function of pH, shown for wild-type hTf/2N (WT) and its H249A, H249E, and H249Q mutants (a) in the absence of chloride and (b) in the presence of chloride. Conditions as described in the text.

be *much* more acid-stable than wild-type, since we have shown crystallographically that the dilysine interaction is not present in H249E. In lactoferrin, for example, the N-lobe binding site also has no dilysine pair, and it appears to be otherwise identical to the equivalent site in transferrin, yet its iron binding is as much as 2 pH units more stable.

The fact that the iron binding in the H249E mutant is only marginally more acid stable than wild-type suggests that either the effect of the dilysine interaction is much smaller than previously believed or that its effect is in some way counterbalanced by the presence of a different ligand (Glu in place of His). In this respect, it is intriguing to note that the acid stability of the H249E mutant is very similar to that of the equivalent mutant of human lactoferrin, H253E (*14*), which loses iron over the pH range 6.0−5.0. Although no crystal structure is available for H253E, it is tempting to speculate that in both cases the Glu is bound to iron as a ligand, that in neither case is a dilysine interaction present, and that their iron binding properties are correspondingly similar. Taking this argument one step further, we note that the mutation H253E *reduced* the acid stability of the lactoferrin site by 1.0−1.5 pH units (*14*), and this probably reflects the change in iron ligation from His to Glu. Thus, we suggest that these two effects operate in the H249E mutant of transferrin—the loss of the dilysine interaction increases acid stability but the change of ligand from His to Glu decreases it, so that the effects almost cancel.

Structural explanations for the data for the other mutants are more difficult to advance, since we do not yet have crystal structures for H249A or H249Q. In the case of H249A, the iron site must be 5-coordinate or have a water molecule as sixth ligand, since no side-chain ligand is available. This should account for its radically more rapid iron release (*21*) and reduced acid stability. Five-coordinate mutants of lactoferrin have been shown to be markedly less stable than wild-type (*14*). The case of H249Q is extremely interesting. There seems to be no structural reason a Gln side chain should not coordinate to iron since it is isostructural with Glu and could in theory coordinate through its amide oxygen. Coordination of a Gln side chain is found in the blue copper protein stellacyanin (*31*), but is rare for transition metal ions in proteins, and the Gln amide oxygen should be a much poorer ligand for Fe^{3+} than the carboxylate oxygen of Glu. In the present case, we note that the acid stability of H249Q is virtually identical to that of H249A, and like H249A, it releases iron dramatically faster than wild-type (*21*). We conclude that although the present H249E crystal structure

MacGillivray et al.

implies that a Gln side chain could coordinate to iron in the H249Q mutant, in fact, it does not, leaving the metal ion either 5-coordinate or with a sixth water ligand. There is a precedent for this in the H253M mutant of the N-lobe half-molecule of lactoferrin, for which the crystal structure shows that Met253 does not coordinate to iron, even though there is no structural impediment, and the iron is 5-coordinate (*14*).

What are the implications for iron binding by transferrins? It appears that proteins of the transferrin family have evolved to operate with a particular set of ligands (2 Tyr, 1 Asp, 1 His, and the carbonate ion) that are ideal for their function of reversible binding of ferric iron. This is reinforced by the apparently convergent evolution of a bacterial ferric-binding protein to a chemically identical set of ligands (*32, 33*). Even though a carboxylate group should be a favorable ligand for Fe(III), the substitution of Glu for His is destabilizing because it disrupts the electroneutrality of the site. Likewise, although a Gln ligand would be neutral like His, it apparently does not coordinate, perhaps because the amide oxygen is too weak a ligand for Fe(III). We note that the insect transferrins (*34, 35*) apparently have Gln in place of His in their N-lobe-binding sites and speculate that this may imply some difference in their requirements for iron binding and release.

CONCLUSIONS

The crystal structure of the H249E mutant of the human transferrin N-lobe half molecule, combined with pH stability data for this and other mutants leads to several important conclusions regarding transferrin function. We observe that the mutated Glu 249 side chain binds to iron (as His 249 does in wild-type) and that Lys 296 moves to hydrogen bond to the noncoordinated carboxylate oxygen of Glu 249; this breaks the dilysine interaction seen in the wild-type protein. We attribute the marginally increased pH stability of the H249E mutant to two opposing factors. Loss of the dilysine interaction makes the protein more acid stable, but the replacement of the uncharged His ligand with a negatively charged Glu ligand counterbalances this. We also conclude that the neutral His ligand thus makes an important contribution to the stability of the canonical transferrin-binding site.

REFERENCES

1. Harris, D. C., and Aisen, P. (1989) in *Iron Carriers and Iron Proteins* (Loehr, T. M., Ed.) pp 241−351, VCH Publishers, New York.
2. Baker, E. N. (1994) *Adv. Inorg. Chem. 41*, 389−463.
3. Klausner, R. D., Ashwell, J. V., Van Renswoude, J. B., Harford, J., and Bridges, K. (1983) *Proc. Natl. Acad. Sci. U.S.A. 80*, 2263−2267.
4. MacGillivray, R. T. A., Mendez, E., Shewale, J. G., Sinha, S. K., Lineback-Zins, J., and Brew, K. (1983) *J. Biol. Chem. 258*, 3543−3553.
5. Bailey, S., Evans, R. W., Garratt, R. C., Gorinsky, B., Hasnain, S., Horsburgh, C., Jhoti, H., Lindley, P. F., Mydin, A., Sarra, R., and Watson, J. L. (1988) *Biochemistry 27*, 5804−5812.
6. Anderson, B. F., Baker, H. M., Dodson, E. J., Norris, G. E., Rumball, S. V., Waters, J. M., and Baker, E. N. (1987) *Proc. Natl. Acad. Sci. U.S.A. 84*, 1769−1773.
7. Anderson, B. F., Baker, H. M., Norris, G. E., Rice, D. W., and Baker, E. N. (1989) *J. Mol. Biol. 209*, 711−734.
8. Kurokawa, H., Mikami, B., and Hirose, M. (1995) *J. Mol. Biol. 254*, 196−207.
9. Woodworth, R. C., Mason, A. B., Funk, W. D., and MacGillivray, R. T. A. (1991) *Biochemistry 30*, 10824−10829.
10. He, Q.-Y., Mason, A. B., Woodworth, R. C., Tam, B. M., Wadsworth, T., and MacGillivray, R. T. A. (1997) *Biochemistry 36*, 5522−5528.
11. He, Q.-Y., Mason, A. B., Woodworth, R. C., Tam, B. M., MacGillivray, R. T. A., Grady, J. K., and Chasteen, N. D. (1997) *Biochemistry 36*, 14853−14860.
12. Zak, O., Aisen, P., Crawley, J. B., Joannou, C. L., Patel, K. J., Rafiq, M., and Evans, R. W. (1995) *Biochemistry 34*, 14428−14434.
13. Faber, H. R., Baker, C. J., Day, C. L., Tweedie, J. W., and Baker, E. N. (1996) *Biochemistry 35*, 14473−14479.
14. Nicholson, H., Anderson, B. F., Bland, T., Shewry, S. C., Tweedie, J. W., and Baker, E. N. (1997) *Biochemistry 36*, 341−346.
15. MacGillivray, R. T. A., Moore, S. A., Chen, J., Anderson, B. F., Baker, H., Luo, Y., Bewley, M., Smith, C. A., Murphy, M. E. P., Wang, Y., Mason, A. B., Woodworth, R. C., Brayer, G. D., and Baker, E. N. (1998) *Biochemistry 37*, 7919−7928.
16. Jeffrey, P. D., Bewley, M. C., MacGillivray, R. T. A., Mason, A. B., Woodworth, R. C., and Baker, E. N. (1998) *Biochemistry 37*, 13978−13986.
17. Anderson, B. F., Baker, H. M., Norris, G. E., Rumball, S. V., and Baker, E. N. (1990) *Nature (London) 344*, 787−790.
18. Bali, P. K., and Aisen, P. (1991) *Biochemistry 30*, 9947−9953.
19. El Hage Chahine, J.-M., and Pakdaman, R. (1995). *Eur. J. Biochem 230*, 1102−1110.
20. Dewan, J. C., Mikami, B., Hirose, M., and Sacchettini, J. C. (1993) *Biochemistry 32*, 11963−11968.
21. He, Q.-Y., Mason, A. B., Dixon, B. K., Tam, B. M., MacGillivray, R. T. A., Pakdaman, R., Chasteen, N. D., and Woodworth, R. C. (1999) *Biochemistry 39*, 1205−1210.
22. Funk, W. D., MacGillivray, R. T. A., Mason, A. B., Brown, S. A., and Woodworth, R. C. (1990) *Biochemistry 29*, 1654−1660.
23. Otwinowski, Z., and Minor, W. (1997) *Methods Enzymol. 276*, 307−326.
24. Collaborative Computing Project 4 (1994) *Acta Crystallogr., Sect. D 50*, 760−763.
25. Brunger, A. T. (1992) X-Plor version 3.1. A System for Crystallography and NMR, Yale University Press, New Haven, CT.
26. Engh, R. A., and Huber, R. (1991) *Acta Crystallogr., Sect. A 47*, 392−400.
27. Jones, T. A., Zou, J.-Y., Cowan, S. W., and Kjeldgaard, M. (1991) *Acta Crystallogr., Sect. A 47*, 110−119.
28. Laskowski, R. A., MacArthur, M. W., Moss, D. S., and Thornton, J. M. (1993) *J. Appl. Crystallogr. 26*, 283−291.
29. Day, C. L., Anderson, B. F., Tweedie, J. W., and Baker, E. N. (1993) *J. Mol. Biol. 232*, 1084−1100.
30. Howard, J. B., and Rees, D. C. (1991) *Adv. Protein Chem. 42*, 199−280.
31. Hart, P. J., Nersissian, A. M., Herrmann, R. G., Nalbandyan, R. M., Valentine, J. S., and Eisenberg, D. (1996) *Protein Sci. 5*, 2175−2183.
32. Bruns, C. M., Nowalk, A. J., Arvai, A. S., McTigue, M. A., Vaughan, K. G., Mietzner, T. A., and McRee, D. E. (1997) *Nat. Struct. Biol. 4*, 919−923.
33. Baker, E. N. (1997) *Nat. Struct. Biol. 4*, 869−871.
34. Bartfeld, N. S., and Law, J. H. (1990) *J. Biol. Chem. 265*, 21684−21691.
35. Jamroz, R. C., Gasdaska, J. R., Bradfield, J. Y., and Law, J. H. (1993) *Proc. Natl. Acad. Sci. U.S.A. 90*, 1320−1324.
36. Kraulis, P. J. (1991) *J. Appl. Crystallogr. 24*, 946−950.
37. Merritt, E. A., and Murphy, M. E. P. (1994) *Acta Crystallogr., Sect. D 50*, 869−873.